ALEPH Tau Spectral Functions and QCD

M. Davier[a], A. Höcker[b], and Z. Zhang[a]

[a]Laboratoire de l'Accélérateur Linéaire, Université Paris-Sud 11, 91898 Orsay, France

[b]Physics Division, CERN, 1211 Geneva 23, Switzerland

Hadronic τ decays provide a clean laboratory for the precise study of quantum chromodynamics (QCD). Observables based on the spectral functions of hadronic τ decays can be related to QCD quark-level calculations to determine fundamental quantities like the strong coupling constant, quark and gluon condensates. Using the ALEPH spectral functions and branching ratios, complemented by some other available measurements, and a revisited analysis of the theoretical framework, the value $\alpha_S(m_\tau^2) = 0.345 \pm 0.004_{\rm exp} \pm 0.009_{\rm th}$ is obtained. Taken together with the determination of $\alpha_S(M_Z^2)$ from the global electroweak fit, this result leads to the most accurate test of asymptotic freedom: the value of the logarithmic slope of $\alpha_s^{-1}(s)$ is found to agree with QCD at a precision of 4%. The value of $\alpha_S(M_Z^2)$ obtained from τ decays is $\alpha_S(M_Z^2) = 0.1215 \pm 0.0004_{\rm exp} \pm 0.0010_{\rm th} \pm 0.0005_{\rm evol} = 0.1215 \pm 0.0012$.

1. Introduction

The τ is the only lepton of the three-generation Standard Model (SM) that is heavy enough to decay into hadrons. It is therefore an ideal laboratory for studying the charged weak hadronic currents and QCD. Observables based on the spectral functions of hadronic τ decays can be related to QCD quark-level calculations to determine fundamental quantities like the strong coupling constant, quark and gluon condensates. We report here the results of a QCD analysis of the final ALEPH spectral functions [1] using a revisited theoretical framework [2].

2. Tau hadronic spectral functions

2.1. Definitions

The spectral function v_1 (a_1, a_0), where the subscript refers to the spin J of the hadronic system, is defined for a nonstrange ($|\Delta S| = 0$) or strange ($|\Delta S| = 1$) vector (axial-vector) hadronic decay $\tau^- \to V^-\nu_\tau$ ($A^-\nu_\tau$). The spectral function is obtained from the normalized invariant mass-squared distribution $(1/N_{V/A})(dN_{V/A}/ds)$ for a given hadronic mass $\sqrt{s}$ multiplied by the appropriate kinematic factor

$$v_1(s)/a_1(s) = \frac{m_\tau^2}{6\,|V_{ud}|^2\,S_{\rm EW}}\,\frac{\mathcal{B}(\tau^- \to V^-/A^-\,\nu_\tau)}{\mathcal{B}(\tau^- \to e^-\,\overline{\nu}_e\nu_\tau)} \times \frac{dN_{V/A}}{N_{V/A}\,ds}\left[\left(1-\frac{s}{m_\tau^2}\right)^2\left(1+\frac{2s}{m_\tau^2}\right)\right]^{-1}, \quad (1)$$

$$a_0(s) = \frac{m_\tau^2}{6\,|V_{ud}|^2\,S_{\rm EW}}\,\frac{\mathcal{B}(\tau^- \to \pi^-(K^-)\,\nu_\tau)}{\mathcal{B}(\tau^- \to e^-\,\overline{\nu}_e\nu_\tau)} \times \frac{dN_A}{N_A\,ds}\left(1-\frac{s}{m_\tau^2}\right)^{-2}, \quad (2)$$

where $S_{\rm EW}$ accounts for electroweak radiative corrections [3]. Since CVC is a very good approximation for the nonstrange sector, the $J = 0$ contribution to the nonstrange vector spectral function is put to zero, while the main contributions to a_0 are from the pion or kaon poles, with $(1/N_A)dN_A/ds = \delta(s - m_{\pi,K}^2)$. They are connected through partial conservation of the axial-vector current (PCAC) to the corresponding decay constants, $f_{\pi,K}$. The spectral functions are normalized by the ratio of the vector/axial-vector branching fraction $\mathcal{B}(\tau^- \to V^-/A^-\nu_\tau)$ to the branching fraction of the massless leptonic, *i.e.*, electron, channel. The direct value for $\mathcal{B}_e$ and the two derived values from $\mathcal{B}_\mu$ and τ_τ using lepton universality are in good agreement with each

other, providing a consistent and precise combined ALEPH result for the electronic branching fraction,

$$\mathcal{B}_e^{\rm uni} = (17.818 \pm 0.032)\% \ . \tag{3}$$

Using unitarity and analyticity, the spectral functions are connected to the imaginary part of the two-point hadronic vacuum polarization functions

$$\Pi^{\mu\nu}_{ij,U} = \left(-g^{\mu\nu}q^2 + q^\mu q^\nu\right)\Pi^{(1)}_{ij,U}(q^2) + q^\mu q^\nu \Pi^{(0)}_{ij,U}(q^2) \tag{4}$$

of vector ($U^\mu_{ij} = V^\mu_{ij} = \overline{q}_j\gamma^\mu q_i$) or axial-vector ($U^\mu_{ij} = A^\mu_{ij} = \overline{q}_j\gamma^\mu\gamma_5 q_i$) color-singlet quark currents, and for time-like momenta-squared $q^2 > 0$. Lorentz decomposition is used to separate the correlation function into its $J = 1$ and $J = 0$ parts. The polarization functions $\Pi^{\mu\nu}_{ij,U}(s)$ have a branch cut along the real axis in the complex $s = q^2$ plane. Their imaginary parts give the spectral functions defined in (1), for nonstrange quark currents

$$\begin{aligned} {\rm Im}\Pi^{(1)}_{ud,V/A}(s) &= \frac{1}{2\pi} v_1/a_1(s) \ , \\ {\rm Im}\Pi^{(0)}_{ud,A}(s) &= \frac{1}{2\pi} a_0(s) \ . \end{aligned} \tag{5}$$

The analytic vacuum polarization function $\Pi^{(J)}_{ij,U}(q^2)$ obeys, up to subtractions, the dispersion relation

$$\Pi^{(J)}_{ij,U}(q^2) = \frac{1}{\pi}\int\limits_0^\infty ds\, \frac{{\rm Im}\Pi^{(J)}_{ij,U}(s)}{s - q^2 - i\varepsilon} \ , \tag{6}$$

where the unknown but in general irrelevant subtraction constants can be removed by taking the derivative of $\Pi_{ij,U}(q^2)$. The dispersion relation allows one to connect the experimentally accessible spectral functions to the correlation functions $\Pi^{(J)}_{ij,U}(q^2)$, which can be derived from QCD.

2.2. Inclusive nonstrange spectral functions

2.2.1. Vector and axial-vector spectral functions

The inclusive τ vector and axial-vector spectral functions are shown in the upper and lower plots of Fig. 1, respectively. The left hand plots give the ALEPH results [5–7] together with its most important exclusive contributions, and the right hand plots compare ALEPH with OPAL [4]. The agreement between the experiments is satisfying.

The curves in the left hand plots of Fig. 1 represent the parton model prediction (dotted) and the massless perturbative QCD prediction (solid), assuming the relevant physics to be governed by short distances. The difference between the two curves is due to higher order terms in the strong coupling $(\alpha_s(s)/\pi)^n$ with $n = 1, 2, 3$. At high energies the spectral functions are assumed to be dominated by continuum production, which locally agrees with perturbative QCD. This asymptotic region is not yet reached at $s = m_\tau^2$ for the vector and axial-vector spectral functions.

2.2.2. Inclusive $V \pm A$ spectral functions

For the total $v_1 + a_1$ hadronic spectral function it is not necessary to experimentally distinguish whether a given event belongs to one or the other current. The one, two and three-pion final states dominate and their exclusive measurements are added with proper accounting for anticorrelations due to the feedthrough. The remaining contributing topologies are treated inclusively, *i.e.*, without separation of the vector and axial-vector decay modes. This reduces the statistical uncertainty. The effect of the feed-through between τ final states on the invariant mass spectrum is described by the Monte Carlo simulation and resolution effects are corrected by data unfolding. In this procedure the simulated mass distributions are iteratively corrected using the exclusive vector/axial-vector unfolded mass spectra. Also, one does not have to separate the vector/axial-vector currents of the $K\overline{K}\pi$ and $K\overline{K}\pi\pi$ modes. The $v_1 + a_1$ spectral functions for ALEPH and OPAL are plotted in the left hand plot of Fig. 2. The improvement in precision when comparing to a sum of the two parts in Fig. 1 is significant at higher mass-squared values.

One nicely identifies the oscillating behavior of the spectral function and it is interesting to observe that, unlike the vector/axial-vector spectral functions, it does approximately reach the asymptotic limit predicted by perturbative QCD

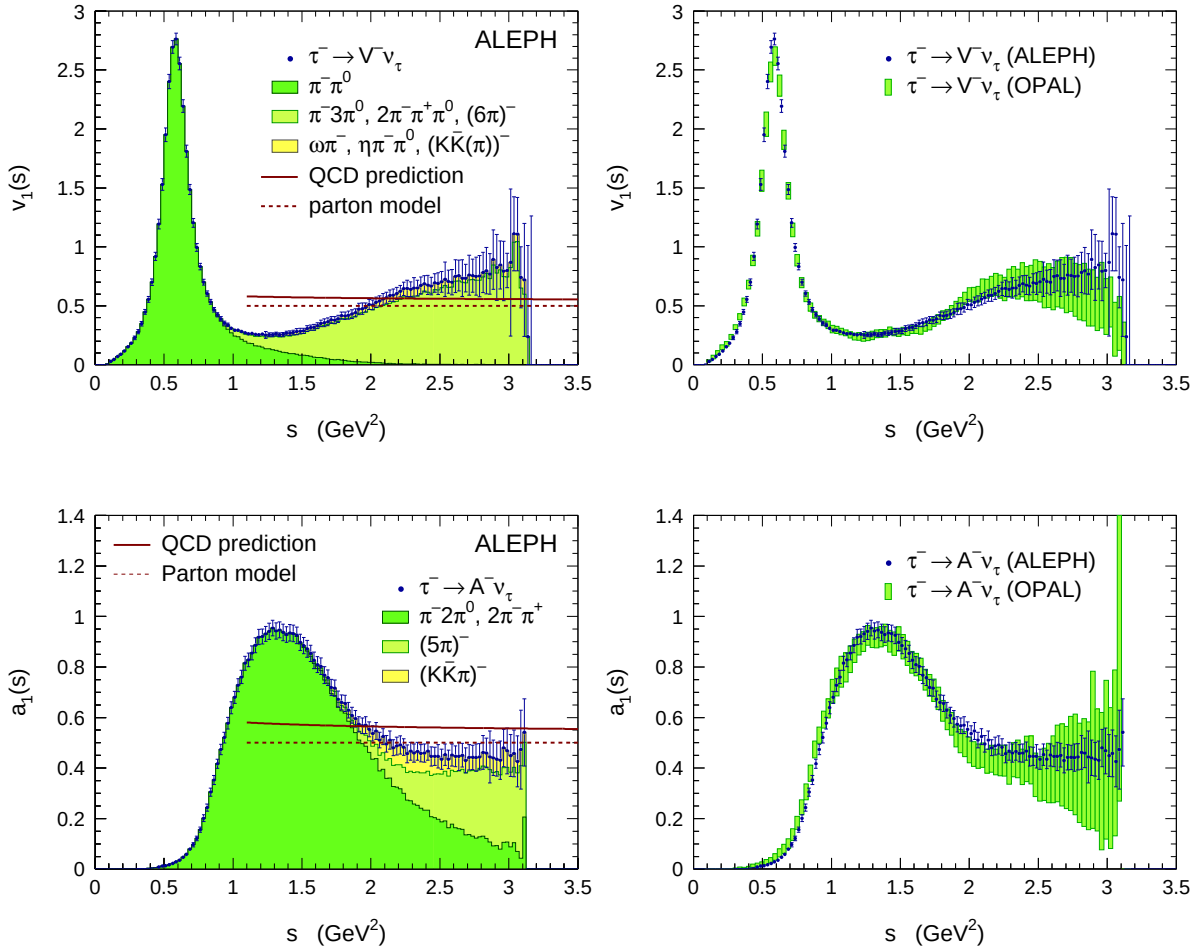

Figure 1. Left hand plots: the inclusive vector (upper) and axial-vector (lower) spectral functions as measured in [5]. The shaded areas indicate the contributing exclusive τ decay channels. The curves show the predictions from the parton model (dotted) and from massless perturbative QCD using $\alpha_s(M_Z^2) = 0.120$ (solid). Right hand plots: comparison of the inclusive vector (upper) and axial-vector (lower) spectral functions obtained by ALEPH and OPAL [4].

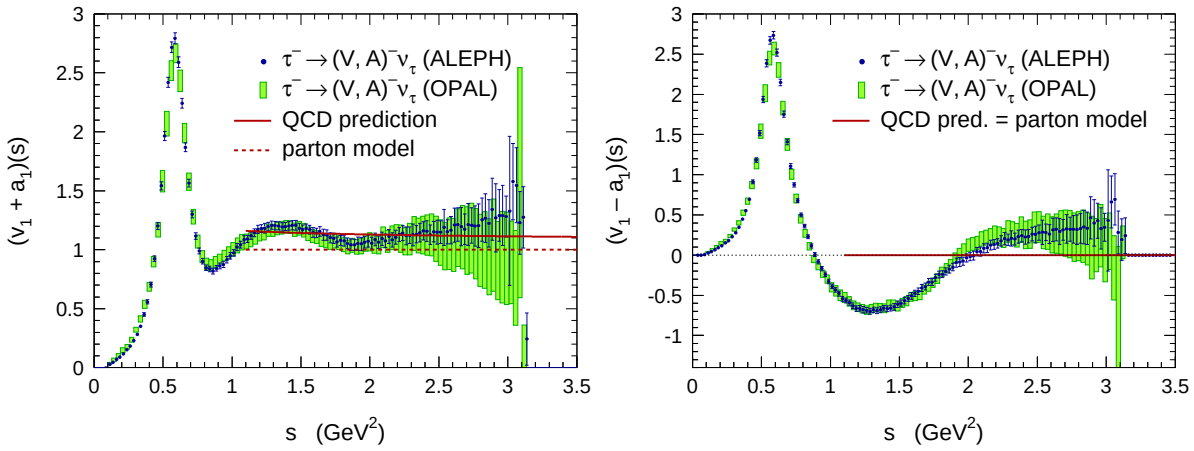

Figure 2. Inclusive vector plus axial-vector (left) and vector minus axial-vector spectral function (right) as measured in [5] (dots with errors bars) and [4] (shaded one standard deviation errors). The lines show the predictions from the parton model (dotted) and from massless perturbative QCD using $\alpha_s(M_Z^2) = 0.120$ (solid). They cancel to all orders in the difference.

at $s \to m_\tau^2$. Also, the $V + A$ spectral function, including the pion pole, exhibits the features expected from global quark-hadron duality: despite the huge oscillations due to the prominent π, $\rho(770)$, a_1 and $\rho(1450)$ resonances, the spectral function qualitatively averages out to the quark contribution from perturbative QCD.

In the case of the $v_1 - a_1$ spectral function, uncertainties on the V/A separation are reinforced due to their relative anticorrelation. Similarly, the presence of anticorrelations in the branching fractions between τ final states with adjacent numbers of pions increase the errors. The $v_1 - a_1$ spectral functions for ALEPH and OPAL are shown in the right hand plot of Fig. 2. The oscillating behavior of the respective v_1 and a_1 spectral functions is emphasized and the asymptotic regime is not reached at $s = m_\tau^2$. However again, the strong oscillation generated by the hadron resonances to a large part averages out to zero, as predicted by perturbative QCD.

3. HADRONIC TAU DECAYS AND QCD

3.1. Generalities

Proposed tests of QCD at the τ mass scale [8–11] and the precise measurement of the strong coupling constant α_s, carried out for the first time by the ALEPH [12] and CLEO [13] collaborations have triggered many theoretical developments. They concern primarily the perturbative expansion for which innovative optimization procedures have been suggested. Among these are contour-improved (resummed) fixed-order perturbation theory [14,15], effective charge and minimal sensitivity schemes [16,17], the large-β_0 expansion [18,19], and combinations of these approaches. They mainly distinguish themselves in how they deal with the fact that the perturbative series is truncated at an order where the missing part is not expected to be small.

One could wonder how τ decays may at all allow us to learn something about perturbative QCD. The hadronic decay of the τ is dominated by resonant single particle final states. The corresponding QCD interactions that bind the quarks and gluons into these hadrons necessarily involve long distance scales, which are outside the domain

of perturbation theory. Indeed, it is the inclusive character of the sum of all hadronic τ decays that allows us to probe fundamental short distance physics. Inclusive observables like the total hadronic τ decay rate R_τ can be accurately predicted as function of $\alpha_s(m_\tau^2)$ using perturbative QCD, and including small nonperturbative contributions within the framework of the Operator Product Expansion (OPE) [20]. In effect, R_τ is a doubly inclusive observable since it is the result of a summation over all hadronic final states at a given invariant mass and further over all masses between m_π and m_τ. The scale m_τ lies in a compromise region where $\alpha_s(m_\tau^2)$ is large enough so that R_τ is sensitive to its value, yet still small enough so that the perturbative expansion converges safely and nonperturbative power corrections are small.

If strong and electroweak radiative corrections are neglected, the theoretical parton level prediction for $SU_C(N_C)$, $N_C = 3$ reads

$$R_\tau = N_C \left(|V_{ud}|^2 + |V_{us}|^2\right) = 3 \ , \qquad (7)$$

and we can estimate a perturbative correction to this value of approximately 21%. One realizes the increase in sensitivity to α_s compared to the Z hadronic width, where because of the three times smaller $\alpha_s(M_Z^2)$ the perturbative QCD correction reaches only about 4%.

The nonstrange inclusive observable R_τ can be theoretically separated into contributions from specific quark currents, namely vector (V) and axial-vector (A) $\overline{u}d$ and $\overline{u}s$ quark currents. It is therefore appropriate to decompose

$$R_\tau = R_{\tau,V} + R_{\tau,A} + R_{\tau,S} \ , \qquad (8)$$

where for the strange hadronic width $R_{\tau,S}$ vector and axial-vector contributions are so far not separated because of the lack of the corresponding experimental information for the Cabibbo-suppressed modes. Parton-level and perturbative terms do not distinguish vector and axial-vector currents (for massless partons). Thus the corresponding predictions become $R_{\tau,V/A} = (N_C/2)|V_{ud}|^2$ and $R_{\tau,S} = N_C|V_{us}|^2$, which add up to Eq. (7).

A crucial issue of the QCD analysis at the τ mass scale is the reliability of the theoretical description, *i.e.*, the use of the OPE to organize the perturbative and nonperturbative expansions, and the control of unknown higher-order terms in these series. A reasonable stability test is to continuously vary m_τ to lower values $\sqrt{s_0} \leq m_\tau$ for both theoretical prediction and measurement, which is possible since the shapes of the τ spectral functions are available. The kinematic factor that takes into account the τ phase space suppression at masses near to m_τ is correspondingly modified so that $\sqrt{s_0}$ represents the new mass of the τ.

3.2. Theoretical prediction of R_τ

According to Eq. (5) the absorptive parts of the vector and axial-vector two-point correlation functions $\Pi^{(J)}_{ud,V/A}(s)$, with the spin J of the hadronic system, are proportional to the τ hadronic spectral functions with corresponding quantum numbers. The nonstrange ratio $R_{\tau,V+A}$ can therefore be written as an integral of these spectral functions over the invariant mass-squared s of the final state hadrons [10]

$$R_{\tau,V+A}(s_0) \, = \, 12\pi S_{\rm EW} \int\limits_0^{s_0} \frac{ds}{s_0} \left(1 - \frac{s}{s_0}\right)^2 \times \qquad (9)$$

$$\left[\left(1 + 2\frac{s}{s_0}\right) {\rm Im}\Pi^{(1)}(s+i\epsilon) \, + \, {\rm Im}\Pi^{(0)}(s+i\epsilon)\right] \ ,$$

where $\Pi^{(J)}$ can be decomposed as $\Pi^{(J)} = |V_{ud}|^2 \left(\Pi^{(J)}_{ud,V} + \Pi^{(J)}_{ud,A}\right)$. The lower integration limit is zero because the pion pole is at zero mass in the chiral limit.

The correlation function $\Pi^{(J)}$ is analytic in the complex s plane everywhere except on the positive real axis where singularities exist. Hence by Cauchy's theorem, the imaginary part of $\Pi^{(J)}$ is proportional to the discontinuity across the positive real axis

$$\int\limits_0^{s_0} ds \, w(s) {\rm Im}\Pi(s) = -\frac{1}{2i} \oint\limits_{|s|=s_0} ds \, w(s) \Pi(s) \ , \qquad (10)$$

where $w(s)$ is an arbitrary analytic function, and the contour integral runs counter-clockwise around the circle from $s = s_0 + i\epsilon$ to $s = s_0 - i\epsilon$ as indicated in Fig. 3.

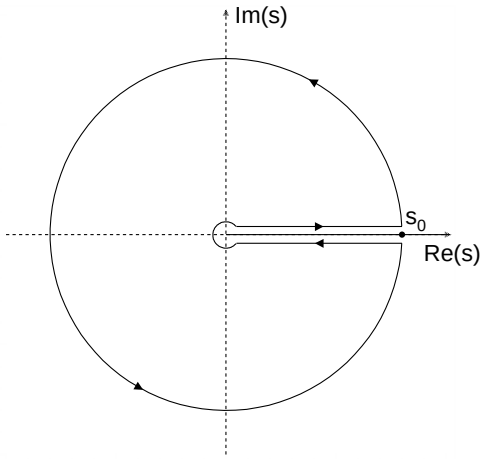

Figure 3. Integration contour for the r.h.s. in Eq. (10).

The energy scale $s_0 = m_\tau^2$ is large enough that contributions from nonperturbative effects are expected to be subdominant and the use of the OPE is appropriate. The kinematic factor $(1 - s/s_0)^2$ suppresses the contribution from the region near the positive real axis where $\Pi^{(J)}(s)$ has a branch cut and the OPE validity is restricted due to large possible quark-hadron duality violations.

The theoretical prediction of the vector and axial-vector ratio $R_{\tau,V/A}$ can hence be written as

$$R_{\tau,V/A} = \frac{3}{2}|V_{ud}|^2 S_{\rm EW} \left(1 + \delta^{(0)} + \delta'_{\rm EW} + \delta^{(2,m_q)}_{ud,V/A} + \sum_{D=4,6,\ldots} \delta^{(D)}_{ud,V/A}\right) , \quad (11)$$

with the massless perturbative contribution $\delta^{(0)}$, the residual non-logarithmic electroweak correction $\delta'_{\rm EW} = 0.0010$ [21], and the dimension $D = 2$ *perturbative* contribution $\delta^{(2,m_q)}_{ud,V/A}$ from quark masses. The term $\delta^{(D)}$ denotes the OPE contributions of mass dimension D

$$\delta^{(D)}_{ud,V/A} = \sum_{\dim\mathcal{O}=D} C_{ud,V/A}(s,\mu) \frac{\langle \mathcal{O}_{ud}(\mu)\rangle_{V/A}}{(-\sqrt{s_0})^D} , \quad (12)$$

where the scale parameter μ separates the long-distance nonperturbative effects, absorbed into the vacuum expectation elements $\langle \mathcal{O}_{ud}(\mu)\rangle$, from the short-distance effects that are included in the Wilson coefficients $C_{ud,V/A}(s,\mu)$. Note that $\delta^{(D)}_{ud,V+A} = (\delta^{(D)}_{ud,V} + \delta^{(D)}_{ud,A})/2$.

3.2.1. The Perturbative Prediction

The perturbative prediction used by the experiments follows the work of [14]. Effects from quark masses have been calculated in [22] and are found to be well below 1% for the light quarks. As a consequence, the contributions from vector and axial-vector currents coincide to any given order of perturbation theory and the results are flavor independent.

For the evaluation of the perturbative series, it is convenient to introduce the analytic Adler function

$$D(s) \equiv -s\frac{d\Pi(s)}{ds} . \quad (13)$$

The function $D(s)$, calculated in perturbative QCD within the $\overline{\rm MS}$ renormalization scheme, depends on a non-physical parameter μ occurring as $\ln(\mu^2/s)$. Furthermore it is a function of α_s. On the other hand, since $D(s)$ is connected to a physical quantity, the spectral function $\mathrm{Im}\Pi(s)$, it cannot depend on the subjective choice of μ. This can be achieved if α_s becomes a function of μ providing independence of $D(s)$ of the choice of μ. Nevertheless, in the realistic case of a truncated series, some μ dependence remains and represents an irreducible systematic uncertainty.

The s dependence of the QCD coupling constant is obtained from the renormalization group equation (RGE)

$$\frac{da_s}{d\ln s} = \beta(a_s) = -a_s^2 \sum_n \beta_n a_s^n , \quad (14)$$

with $a_s = \alpha_s/\pi$. Expressed in the $\overline{\rm MS}$ renormalization scheme and for three active quark flavors at the τ mass scale, the β_n coefficients are known to four loops ($n = 3$) [23].

The perturbative expansion of the Adler function can be inferred from the 3-loop calculation of the e^+e^- inclusive cross section ratio $R_{e^+e^-}(s) = \sigma(e^+e^- \to \text{hadrons}\,(\gamma))/\sigma(e^+e^- \to$

$\mu^+\mu^-(\gamma)$) [24,25]

$$D(s) = \frac{1}{4\pi^2}\sum_{n=0}^{\infty}\tilde{K}_n(\xi)a_s^n(-\xi s)\ , \qquad (15)$$

where the $\tilde{K}_n(\xi)$ can be expressed [14] as function of K_n and β_n parameters (both known up to order $n=3$), and ξ, an independent scale parameter. This leads to the perturbative expansion

$$\delta^{(0)} = \sum_{n=1}^{5}\tilde{K}_n(\xi)A^{(n)}(a_s)\ , \qquad (16)$$

with the functions

$$A^{(n)}(a_s) = \frac{1}{2\pi i}\oint\limits_{|s|=s_0}\frac{ds}{s}\times \qquad (17)$$
$$\left[1-2\frac{s}{s_0}+2\left(\frac{s}{s_0}\right)^3-\left(\frac{s}{s_0}\right)^4\right]a_s^n(-\xi s)\ .$$

3.2.2. Fixed-order perturbation theory (FOPT)

Inserting the RGE solution for $a_s(s)$ into Eq. (16) to evaluate the contour integral, and collecting the terms with equal powers in a_s leads to the familiar expression [14]

$$\delta^{(0)} = \sum_n\left[\tilde{K}_n(\xi)+g_n(\xi)\right]\left(\frac{\alpha_s(\xi s_0)}{\pi}\right)^n\ , \qquad (18)$$

where the g_n are functions of $\tilde{K}_{m<n}$ and $\beta_{m<n-1}$, and of elementary integrals with logarithms of power $m<n$ in the integrand. Setting $\xi=1$ and replacing all known β_i and K_i coefficients by their numerical values, Eq. (18) simplifies to

$$\begin{aligned}\delta^{(0)} &= a_s(s_0)+(1.6398+3.5625)\,a_s^2(s_0)\\ &\quad+(6.371+19.995)\,a_s^3(s_0)\\ &\quad+(K_4+78.003)\,a_s^4(s_0)\\ &\quad+(K_5+14.250\,K_4-391.54)\,a_s^5(s_0)\ ,\end{aligned} \qquad (19)$$

where for the purpose of systematic studies we have kept terms up to fifth order. When only two numbers are given in the parentheses, the first number corresponds to K_n, and the second to g_n.

The FOPT series is truncated at given order despite the fact that parts of the higher coefficients $g_{n>4}(\xi)$ are known to all orders and could be resummed. These known parts are the higher (up to infinite) order logarithmic power terms of the expansion that are functions of the known $\beta_{n\leq 3}$ and $K_{n\leq 3}$ only. In effect, beyond the use of the perturbative expansion of the Adler function (15), two approximations have been used to obtain the FOPT series (19): *(i)* the RGE (14) has been Taylor-expanded and terms higher than the given FOPT order have been truncated, and *(ii)* this Taylor expansion is used to predict $a_s(-s)$ on the entire $|s|=s_0$ contour.

3.2.3. Contour-improved fixed-order perturbation theory (CIPT)

A more promising approach to the solution of the contour integrals Eq.(17) is to perform a direct numerical evaluation by means of single-step integration and using the solution of the RGE to four loops as input for the running $a_s(-\xi s)$ at each integration step [15,14]. It implicitly provides a partial resummation of the (known) higher order logarithmic integrals and improves the convergence of the perturbative series. While for instance the third order term in the expansion (19) contributes with 17% to the total (truncated) perturbative prediction, the corresponding term of the numerical solution amounts to only 6% (assuming $\alpha_s(m_\tau^2)=0.35$). This numerical solution of Eq. (16) is referred to as *contour-improved* fixed-order perturbation theory (CIPT) in the following. Single-step integration also avoids the Taylor approximation of the RGE on the entire contour, since a_s is iteratively computed from the previous step using the full known RGE.

3.2.4. Other schemes and the value of K_4

Other approaches for evaluating the perturbative prediction have been presented, such as the effective charge perturbation theory (ECPT, see for instance Refs. [16,26]) and the large-β_0 expansion [18,19]. Whereas these methods are of considerable theoretical interest, they are not suited for precision analyses [2].

ECPT has been largely used to estimate the value of the first uncalculated term K_4 [27]. Another approach to estimating K_4 [28] is, within CIPT, to enhance the sensitivity to higher order perturbative terms by reducing the renormaliza-

tion scale ξ. Both methods yield $K_4 \sim 27$, but it has been shown [2] that the precision of this estimate is seriously limited (~ 100 %) by the lack of knowledge of the unknown higher order parameters in the perturbative series ($K_5, \ldots$).

Significant efforts are underway with the goal to calculate the K_4 coefficient. Although the large number of five-loop diagrams that are needed to calculate the two-point current correlator at this order may appear discouraging, the results on two gauge invariant subsets are already available. The subset of order $\mathcal{O}(\alpha_s^4 n_f^3)$ was evaluated long ago through the summation of renormalon chains [29], while the much harder subset $\mathcal{O}(\alpha_s^4 n_f^2)$ was recently calculated [30]. Following these investigations, the value $K_4 = 25 \pm 25$ is used in our analysis.

3.2.5. Comparison of the perturbative methods

To study the convergence of the perturbative series, we give in Table 1 the contributions of the different orders in PT to $\delta^{(0)}$ for the various approaches using $\alpha_s(m_\tau^2) = 0.35$. A geometric growth, $K_n \sim K_{n-1}^2/K_{n-2}$, is assumed for all unknown PT and RGE coefficients. In the case of CIPT the results are given for the various techniques used to evolve $\alpha_s(s)$.

Faster convergence is observed for CIPT compared to FOPT yielding a significantly smaller error associated with the renormalization scale ambiguity. Our coarse extrapolation of the higher order coefficients could indicate that minimal sensitivity is reached at $n \sim 5$ for FOPT, while the series further converges for CIPT. Although the Taylor expansion in the CIPT integral exhibits significant deviations from the exact solution on the integration circle, the actual numerical effect from this on $\delta^{(0)}$ is small (*cf.* second and third column in Table 1). The convergence of the ECPT series is much worse than for FOPT and CIPT. Consequently, the difference between truncation at $n = 4$ and $n = 6$ may be significant. A similar instability may occur for the large-β_0 expansion.

The CIPT series is found to be better behaved than FOPT (as well as ECPT) and is therefore to be preferred for the numerical analysis of the τ hadronic width. As a matter of fact, the difference in the result observed when using a Taylor expansion and when truncating the perturbative series after integrating along the contour (FOPT) with the exact result at given order (CIPT) exhibits the incompleteness of the perturbative series. However, it is even worse than that since large known coefficients are neglected in FOPT so that the difference between CIPT and FOPT may actually overstate the perturbative truncation uncertainty (certainly it is not a good measure of the latter uncertainty). This can be verified by studying the behavior of this difference for the various orders in perturbation theory given in Table 1. The CIPT-vs.-FOPT discrepancy increases with the addition of each order, up to order four where a maximum is reached. Adding the fifth order does not reduce the effect, and only beyond fifth order the two evaluations may become asymptotic to each other. As a consequence varying the unknown higher order coefficients *and* using the difference between FOPT and CIPT as indicator of the theoretical uncertainties overemphasizes the truncation effect.

3.3. Results

It was shown in [11] that one can exploit the shape of the spectral functions to obtain additional constraints on $\alpha_s(s_0)$ and—more importantly—on the nonperturbative effective operators. The τ *spectral moments* at $s_0 = m_\tau^2$ are defined by

$$R_{\tau,V/A}^{k\ell} = \int_0^{m_\tau^2} ds \left(1 - \frac{s}{m_\tau^2}\right)^k \left(\frac{s}{m_\tau^2}\right)^\ell \frac{dR_{\tau,V/A}}{ds} \quad (20)$$

where $R_{\tau,V/A}^{00} = R_{\tau,V/A}$. The factor $(1 - s/m_\tau^2)^k$ suppresses the integrand at the crossing of the positive real axis where the validity of the OPE less certain and the experimental accuracy is statistically limited. Its counterpart $(s/m_\tau^2)^\ell$ projects upon higher energies. The spectral information is used to fit simultaneously $\alpha_s(m_\tau^2)$ and the effective operators $\langle a_s GG\rangle$, $\rho\alpha_s\langle\overline{q}q\rangle^2$ and $\langle\mathcal{O}_D\rangle$ for dimension $D = 4$, 6 and 8, respectively. Due to the large correlations between the differently weighted spectral integrals, only five moments are used as input to the fit.

Table 1
Massless perturbative contribution to $R_\tau(m_\tau^2)$ for the various methods considered, and at orders $n \geq 1$ with $\alpha_s(m_\tau^2) = 0.35$. The value of K_4 is set to 25, while all unknown higher order $K_{n>4}$ and $\beta_{n>3}$ coefficients are assumed to follow a geometric growth. Details are given in Ref. [2].

	δ^0							
Pert. Method	$n=1$	$n=2$	$n=3$	$(n=4)$	$(n=5)$	$(n=6)$	$\sum_{n=1}^{4}$	$\sum_{n=1}^{6}$
FOPT ($\xi=1$)	0.1114	0.0646	0.0365	0.0159	0.0010	−0.0086	0.2283	0.2208
CIPT (Taylor RGE, $\xi=1$)	0.1573	0.0317	0.0126	0.0042	0.0011	0.0001	0.2058	0.2070
CIPT (full RGE, $\xi=1$)	0.1524	0.0311	0.0129	0.0046	0.0013	0.0002	0.2009	0.2025
CIPT (full RGE, $\xi=0.4$)	0.2166	−0.0133	0.0006	−0.0007	0.0010	−0.0007	0.2032	0.2048
ECPT	0.1442	0.2187	−0.1195	−0.0344	−0.0160	−0.0120	0.2090	0.1810
Large-β_0 expansion	0.1114	0.0635	0.0398	0.0241	0.0155	0.0093	0.2388	0.2636

In analogy to R_τ, the contributions to the moments originating from perturbative and nonperturbative QCD are decomposed through the OPE.

3.3.1. The ALEPH determination of $\alpha_s(m_\tau^2)$ and nonperturbative contributions

Combined fits to experimental spectral moments and the extraction of $\alpha_s(m_\tau^2)$ together with the leading nonperturbative operators have been performed by ALEPH, CLEO and OPAL [4,5,7, 12,13] using similar strategies and inputs. This analysis uses the final and complete data on branching fractions and spectral functions from ALEPH [5], yielding

$$R_{\tau,V+A} = 3.482 \pm 0.014 \,, \quad (21)$$
$$R_{\tau,V} = 1.787 \pm 0.011 \pm 0.007 \,, \quad (22)$$
$$R_{\tau,A} = 1.695 \pm 0.011 \pm 0.007 \,, \quad (23)$$
$$R_{\tau,V-A} = 0.092 \pm 0.018 \pm 0.014 \,, \quad (24)$$

where the second error originates from the V/A separation in final states with a $K\overline{K}$ pair, fully anticorrelated beetwen $R_{\tau,V}$ and $R_{\tau,A}$. To reduce the model dependence of the analysis, one fits simultaneously the nonperturbative operators, which is possible since the correlations between these and α_s turn out to be small enough. The main theoretical uncertainties are due to K_4 (25±25) and to the renormalization scale, which is varied around m_τ from 1.1 to 2.5 GeV (the variation over half of the range taken as systematic uncertainty).

The fit results are given in Table 2. There is a remarkable agreement within statistical errors between the $\alpha_s(m_\tau^2)$ determinations using the vector and axial-vector data. This provides an important consistency check of the results, since the two corresponding spectral functions are experimentally independent and manifest a quite different resonant behavior. However it must be mentioned that the $\alpha_s(m_\tau^2)$ determination using either the V and A spectral functions is more dependent on the validity of the OPE approach since their nonperturbative contributions are significantlty larger than for $V+A$. Indeed the leading nonperturbative contributions of dimension $D = 6$ and $D = 8$ approximately cancel in the inclusive sum. This cancellation of the nonperturbative terms increases the confidence in the $\alpha_s(m_\tau^2)$ determination from the inclusive $V + A$ observables. Averaging CIPT and FOPT, the result quoted by ALEPH is

$$\alpha_s(m_\tau^2) = 0.340 \pm 0.005_{\rm exp} \pm 0.014_{\rm th} \,, \quad (25)$$

The gluon condensate is determined by the first $k = 1$, $\ell = 0, 1$ moments, which receive lowest order contributions. The values obtained in the V and A fits are not very consistent, which could indicate problems in the validity of the OPE approach used once the nonperturbative terms become significant. Taking the value obtained in the $V+A$ fit, where nonperturbative effects are small, and adding as systematic uncertainties half of the

Table 2
Results [5] for $\alpha_s(m_\tau^2)$ and the nonperturbative contributions for vector, axial-vector and $V+A$ combined fits using the corresponding experimental spectral moments as input parameters. Where two errors are given the first is experimental and the second theoretical. The $\delta^{(2)}$ term is theoretical only with quark masses varying within their allowed ranges (see Ref. [2]). The quark condensates in the $\delta^{(4)}$ term are obtained from PCAC, while the gluon condensate is determined by the fit. The total nonperturbative contribution is the sum $\delta_{\rm NP} = \delta^{(4)} + \delta^{(6)} + \delta^{(8)}$. Full results are listed only for the CIPT perturbative prescription, except for $\alpha_s(m_\tau^2)$ where the results using both CIPT and FOPT are given (See Ref. [1] for the complete results).

Parameter	Vector (V)	Axial-Vector (A)	$V + A$
$\alpha_s(m_\tau^2)$ (CIPT)	$0.355 \pm 0.008 \pm 0.009$	$0.333 \pm 0.009 \pm 0.009$	$0.350 \pm 0.005 \pm 0.009$
$\alpha_s(m_\tau^2)$ (FOPT)	$0.331 \pm 0.006 \pm 0.012$	$0.327 \pm 0.007 \pm 0.012$	$0.331 \pm 0.004 \pm 0.012$
$\delta^{(2)}$ (CIPT)	$(-3.3 \pm 3.0) \times 10^{-4}$	$(-5.1 \pm 3.0) \times 10^{-4}$	$(-4.4 \pm 2.0) \times 10^{-4}$
$\langle a_s GG \rangle$ (GeV^4) (CIPT)	$(0.4 \pm 0.3) \times 10^{-2}$	$(-1.3 \pm 0.4) \times 10^{-2}$	$(-0.5 \pm 0.3) \times 10^{-2}$
$\delta^{(4)}$ (CIPT)	$(4.1 \pm 1.2) \times 10^{-4}$	$(-5.7 \pm 0.1) \times 10^{-3}$	$(-2.7 \pm 0.1) \times 10^{-3}$
$\delta^{(6)}$ (CIPT)	$(2.85 \pm 0.22) \times 10^{-2}$	$(-3.23 \pm 0.26) \times 10^{-2}$	$(-2.1 \pm 2.2) \times 10^{-3}$
$\delta^{(8)}$ (CIPT)	$(-9.0 \pm 0.5) \times 10^{-3}$	$(8.9 \pm 0.6) \times 10^{-3}$	$(-0.3 \pm 4.8) \times 10^{-4}$
Total $\delta_{\rm NP}$ (CIPT)	$(1.99 \pm 0.27) \times 10^{-2}$	$(-2.91 \pm 0.20) \times 10^{-2}$	$(-4.8 \pm 1.7) \times 10^{-3}$
χ^2/DF (CIPT)	0.52	4.97	3.66

difference between the vector and axial-vector fits as well as between the CIPT and FOPT results, ALEPH measures the gluon condensate to be

$$\langle a_s GG \rangle = (0.001 \pm 0.012)\,\text{GeV}^4. \qquad (26)$$

This result does not provide evidence for a nonzero gluon condensate, but it is consistent with and has comparable accuracy to the independent value obtained using charmonium sum rules and e^+e^- data in the charm region, $(0.011 \pm 0.009)\,\text{GeV}^4$ in a combined determination with the c quark mass [31].

The approximate cancellation of the nonperturbative contributions in the $V + A$ case was predicted [10] for $D = 6$ assuming vacuum saturation for the matrix elements of four-quark operators, which yields $\delta_V^{(6)}/\delta_A^{(6)} = -7/11 = -0.64$, in fair agreement with the result -0.90 ± 0.18. The estimate [10] for $\delta_V^{(6)} = (2.5 \pm 1.3) \times 10^{-2}$ agrees with the experimental result.

The total nonperturbative $V + A$ correction, $\delta_{{\rm NP},V+A} = (-4.3 \pm 1.9) \times 10^{-3}$, is an order of magnitude smaller than the corresponding values in the V and A components, $\delta_{{\rm NP},V} = (2.0 \pm 0.3) \times 10^{-2}$ and $\delta_{{\rm NP},A} = (-2.8 \pm 0.3) \times 10^{-2}$.

3.3.2. Running of $\alpha_s(s)$ below m_τ^2

Using the spectral functions, one can simulate the physics of a hypothetical τ lepton with a mass $\sqrt{s_0}$ smaller than m_τ through Eq. (9). Assuming quark-hadron duality, the evolution of $R_\tau(s_0)$ provides a direct test of the running of $\alpha_s(s_0)$, governed by the RGE β-function. On the other hand, it is also a test of the stability of the OPE approach at small scales. The studies performed in this section employ only CIPT.

The measured function $R_{\tau,V+A}(s_0)$ is plotted in the left hand plot of Fig. 4 together with the theoretical prediction using the results of Table 2. The correlations between two adjacent points in s_0 are large as the only new information is provided by the small mass difference between the two points and the slightly modified weight functions under the integral. Moreover the correla-

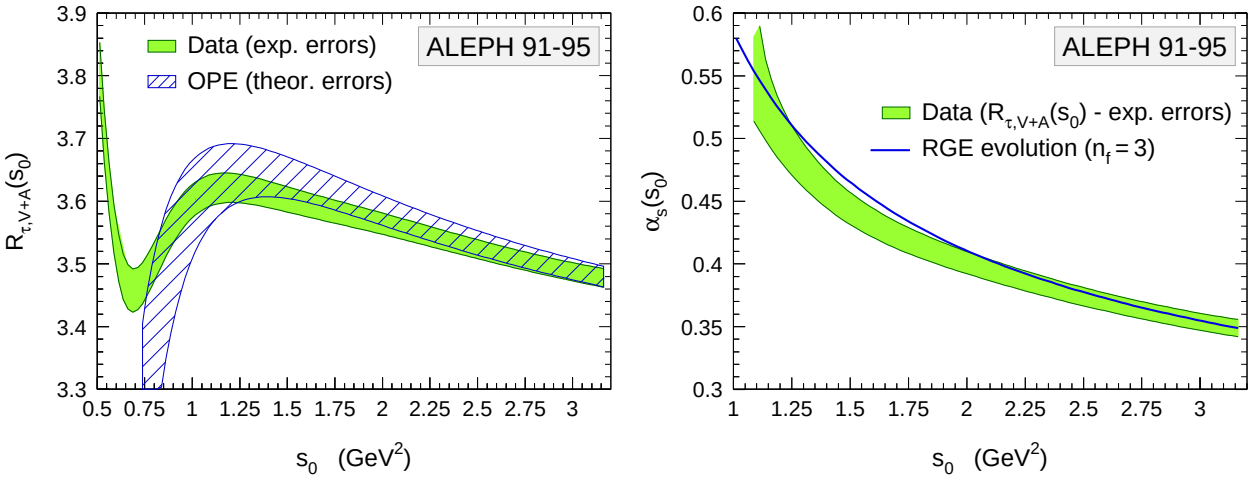

Figure 4. Left: The ratio $R_{\tau,V+A}$ versus the square "τ mass" s_0. The curves are plotted as error bands to emphasize their strong point-to-point correlations in s_0. Also shown is the theoretical prediction using CIPT and the results for $R_{\tau,V+A}$ and the nonperturbative terms from Table 2. Right: The running of $\alpha_s(s_0)$ obtained from the fit of the theoretical prediction to $R_{\tau,V+A}(s_0)$ using CIPT. The shaded band shows the data including only experimental errors. The curve gives the expected four-loop RGE evolution for three flavors.

tions are reinforced by the original experimental and theoretical correlations. Below 1 GeV^2 the error of the theoretical prediction of $R_{\tau,V+A}(s_0)$ starts to blow up because of the increasing sensitivity to the unknown K_4 perturbative term; errors of the nonperturbative contributions are *not* contained in the theoretical error band. Figure 4 (right) shows the plot corresponding to Fig. 4 (left), translated into the running of $\alpha_s(s_0)$. Only experimental errors are shown. Also plotted is the four-loop RGE evolution using three quark flavors.

It is remarkable that the theoretical prediction using the parameters determined at the τ mass and $R_{\tau,V+A}(s_0)$ extracted from the measured $V + A$ spectral function agree down to $s_0 \sim 0.8\,\text{GeV}^2$. The agreement is good to about 2% at 1 GeV^2. This result, even more directly illustrated by the right hand plot of Fig. 4, demonstrates the validity of the perturbative approach down to masses around 1 GeV, well below the τ mass scale. The agreement with the expected scale evolution between 1 and 1.8 GeV is an interesting result, considering the relatively low mass range, where α_s is seen to decrease by a factor of 1.6 and reaches rather large values ~ 0.55 at the lowest masses. This behavior provides confidence that the $\alpha_s(m_\tau^2)$ measurement is on solid phenomenological ground.

3.3.3. Final assessment on the $\alpha_s(m_\tau^2)$ determination

Although this evaluation of $\alpha_s(m_\tau^2)$ represents the state-of-the art, several remarks can be made:

- The analysis is based on the ALEPH spectral functions and branching fractions, ensuring a good consistency between all the observables, but not exploiting the full experimental information currently available from other experiments. Because the result on $\alpha_s(m_\tau^2)$ is limited by theoretical uncertainties, one should expect only a small improvement of the final error in this way, however it can influence the central value.

- One example for this is the evaluation of the strange component. Some discrepancy

is observed between the ALEPH measurement of the $(K\pi\pi)^-\nu$ mode and the CLEO and OPAL results. Although this could still be the result of a statistical fluctuation, their average provides a significant shift in the central value compared to using the ALEPH number alone. Another improvement is the substitution of the measured branching fraction for the $K^-\nu$ mode by the more precise value predicted from τ–μ universality. Both operations have the effect to increase $R_{\tau,S}$, the ratio of the τ decay width into strange hadronic final states to the electronic width, from 0.1603 ± 0.0064, as obtained by ALEPH, to 0.1686 ± 0.0047 for the world average.

- One can likewise substitute the world average value for the universality-improved value of the electronic branching fraction, $\mathcal{B}_e^{\rm uni} = (17.818 \pm 0.032)\%$, to the ALEPH result, $\mathcal{B}_e = (17.810 \pm 0.039)\%$, with little change in the central value, but some improvement in the precision.

From this analysis, one finds the new value for the nonstrange ratio,

$$\begin{aligned} R_{\tau,V+A} &= R_\tau - R_{\tau,S} \\ &= (3.640 \pm 0.010) - (0.1686 \pm 0.0047) \\ &= 3.471 \pm 0.011 \ . \end{aligned} \tag{27}$$

The result (27) translates into the following determination of $\alpha_s(m_\tau^2)$ from the inclusive $V + A$ component using the CIPT approach

$$\alpha_s(m_\tau^2) = 0.345 \pm 0.004_{\rm exp} \pm 0.009_{\rm th} \ , \tag{28}$$

with improved experimental and theoretical precision over the ALEPH result. Most of the theoretical uncertainty originates from the limited knowledge of the perturbative expansion, only predicted to third order. Following the dicussion above we take the result from the CIPT expansion, not introducing any additional uncertainty spanning the difference between FOPT and CIPT results. The dominant theoretical errors are from the uncertainty on K_4 and from the renormalization scale dependence, both covering the effect of truncating the series after the estimated fourth order.

3.3.4. Evolution to M_Z^2

It is customary to compare α_s values, obtained at different renormalization scales, at the scale of the Z-boson mass.

The evolution of the $\alpha_s(m_\tau^2)$ measurement from the inclusive $V + A$ observables given in Eq. (28), based on Runge-Kutta integration of the RGE (14) to N^{3}LO , and three-loop quark-flavor matching, gives

$$\begin{aligned} \alpha_s(M_Z^2) &= 0.1215 \ (4_{\rm exp}) \ (10)_{\rm th} \ (5)_{\rm evol} \ , \\ &= 0.1215 \pm 0.0012 \ . \end{aligned} \tag{29}$$

The first two errors originate from the $\alpha_s(m_\tau^2)$ determination given in Eq. (28). The last error receives contributions from the uncertainties in the c-quark mass (0.00020, m_c varied by $\pm 0.1\,$GeV) and the b-quark mass (0.00005, m_b varied by $\pm 0.1\,$GeV), the matching scale (0.00023, μ varied between $0.7\,m_q$ and $3.0\,m_q$), the three-loop truncation in the matching expansion (0.00026) and the four-loop truncation in the RGE equation (0.00031), where we used for the last two errors the size of the highest known perturbative term as systematic uncertainty. These errors have been added in quadrature. The result (29) is a determination of the strong coupling at the Z mass scale with a precision of 1%.

The evolution path of $\alpha_s(m_\tau^2)$ is shown in the upper plot of Fig. 5. The two discontinuities are due to the quark-flavor matching at $\mu = 2m_q$. One could prefer to have an (almost) smooth matching by choosing $\mu = m_q$. However, in this case, one must first evolve from m_τ down to $\overline{m}_c$ to match the c-quark flavor, before evolving to $\overline{m}_b$. The effect on $\alpha_s(M_Z^2)$ from this ambiguity is within the assigned systematic uncertainty for the evolution.

The comparison with the other determinations of $\alpha_s(M_Z^2)$ is given in Fig. 5 using compiled results from Ref. [32].

3.3.5. A measure of asymptotic freedom between m_τ^2 and M_Z^2

The τ-decay and Z-width determinations have comparable accuracies, which are however very different in nature. The τ value is dominated by theoretical uncertainties, whereas the determination at the Z resonance, benefiting from the much

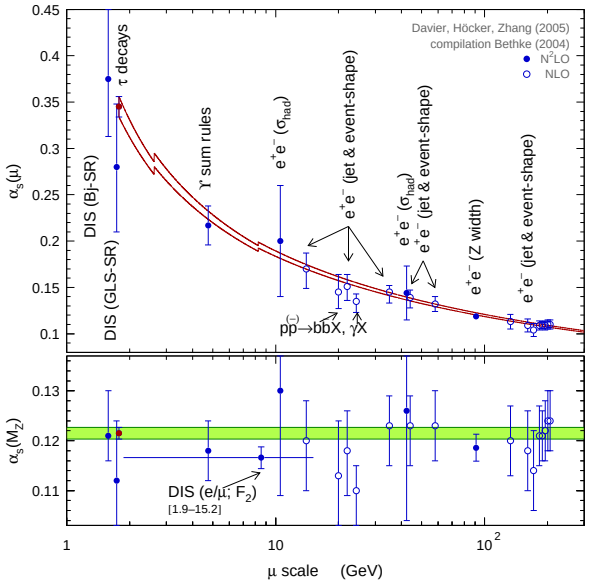

Figure 5. Top: The evolution of $\alpha_S(m_\tau^2)$ (28) to higher scales μ using the four-loop RGE and the 3-loop matching conditions applied at the heavy quark-pair thresholds (hence the discontinuities at $2m_c$ and $2m_b$). The evolution is compared with other independent measurements (see text) covering scales varying over more than two orders magnitude. The experimental values are taken from the compilation [32]. Bottom: The corresponding extrapolated α_S values at M_Z. The shaded band displays the τ decay result within errors.

larger energy scale and the correspondingly small uncertainties from the truncated perturbative expansion, is limited by the experimental precision on the electroweak observables, essentially the ratio of leptonic to hadronic peak cross sections. The consistency between the two results provides the most powerful present test of the evolution of the strong interaction coupling, as it is predicted by the nonabelian nature of the QCD gauge theory. This test extends over a range of s spanning more than three orders of magnitude. The difference between the extrapolated τ-decay value and the measurement at the Z is:

$$\alpha_S^\tau(M_Z^2) - \alpha_S^Z(M_Z^2) = 0.0029\ (10)_\tau\ (27)_Z \qquad (30)$$

which agrees with zero with a relative precision of 2.4%.

In fact, the comparison of these two values is valuable since they are among the most precise single measurements and they are widely spaced in energy scale. Thus it allows one to perform an accurate test of asymptotic freedom. Let us consider the following evolution estimator [33] for the inverse of $\alpha_S(s)$,

$$r(s_1, s_2) = 2 \cdot \frac{\alpha_S^{-1}(s_1) - \alpha_S^{-1}(s_2)}{\ln s_1 - \ln s_2}\ , \qquad (31)$$

which reduces to the logarithmic derivative of $\alpha_S^{-1}(s)$ when $s_1 \to s_2$,

$$\frac{d\alpha_S^{-1}}{d\ln\sqrt{s}} = -\frac{2\pi\beta(s)}{\alpha_S^2}\ , \quad = \frac{2\beta_0}{\pi}\left(1 + \frac{\beta_1}{\beta_0}\frac{\alpha_S}{\pi} + \cdots\right)\ , \qquad (32)$$

with the notations of Eq. (14). At first order, the logarithmic derivative is driven by β_0.

The τ and Z experimental determinations of $\alpha_S(s)$ yield the value

$$r_{\rm exp}(m_\tau^2, M_Z^2) = 1.405 \pm 0.053\ , \qquad (33)$$

which agrees with the prediction using the RGE to N^{3}LO, and 3-loop quark-flavor matching,

$$r_{\rm QCD}(m_\tau^2, M_Z^2) = 1.353 \pm 0.006\ . \qquad (34)$$

To our knowledge this is the most precise experimental test of the asymptotic freedom property of QCD at present. It can be compared to an independent determination [33], using an analysis of event shape observables at LEP between the Z energy and 207 GeV, $r(M_Z^2, (207\ \text{GeV})^2) = 1.11 \pm 0.21$, for a QCD expectation of 1.27.

4. Conclusions

Using the ALEPH spectral functions and branching ratios, complemented by other available measurements, and a revisited analysis of the theoretical framework, the value $\alpha_S(m_\tau^2) = 0.345 \pm 0.004_{\rm exp} \pm 0.009_{\rm th}$ is obtained. Taken together with the determination of $\alpha_S(M_Z^2)$ from the global electroweak fit, this result leads to the most accurate test of asymptotic freedom: the value of the logarithmic slope of $\alpha_s^{-1}(s)$ is found to agree with QCD at a precision of 4%.

REFERENCES

1. ALEPH Collaboration (S. Schael et al.), Phys. Rep., 421 (2005) 191.
2. M. Davier, A. Höcker, and Z. Zhang, Rev. Mod. Phys., 78 (2006).
3. W. Marciano and A. Sirlin, Phys. Rev. Lett., 61 (1988) 1815.
4. OPAL Collaboration (K. Ackerstaff et al.) Eur. Phys. J. C7 (1999) 571.
5. ALEPH Collaboration (D. Buskulic et al.), Z. Phys., C70 (1996) 561; 579.
6. ALEPH Collaboration (D. Buskulic et al.), Z. Phys., C76 (1997) 15.
7. ALEPH Collaboration (D. Buskulic et al.), Eur. Phys. J., C4 (1998) 409.
8. S. Narison and A. Pich, Phys. Lett., B211 (1988) 183.
9. E. Braaten, Phys. Rev., D39 (1989) 1458.
10. E. Braaten, S. Narison, and A. Pich, Nucl. Phys., B373 (1992) 581.
11. F. LeDiberder and A. Pich, Phys. Lett., B289 (1992) 165.
12. ALEPH Collaboration (D. Buskulic et al.), Phys. Lett., B307 (1993) 209.
13. CLEO Collaboration (T. Coan et al.), Phys. Lett., B356 (1995) 580.
14. F. LeDiberder and A. Pich, Phys. Lett., B286 (1992) 147.
15. A. A. Pivovarov, Sov. J. Nucl. Phys., 54 (1991) 676; Z. Phys., C53 (1992) 461.
16. G. Grunberg, Phys. Lett., B95 (1980) 70.
17. P. S. Stevenson, Phys. Rev., D23 (1981) 2916.
18. P. Ball, M. Beneke, and V. M. Braun, Nucl. Phys., B452 (1995) 563.
19. M. Neubert, Nucl. Phys., B463 (1996) 511.
20. M. A. Shifman, A. L. Vainshtein, and V. I. Zakharov, Nucl. Phys., B147 (1979) 385; 448 ; 519.
21. E. Braaten and C. S. Li, Phys. Rev., D42 (1990) 3888.
22. K. G. Chetyrkin and A. Kwiatkowski, Z. Phys., C59 (1993) 525.
23. T. van Ritbergen, J. A. M. Vermaseren, and S.A. Larin, Phys. Lett., B400 (1997) 379.
24. M. Dine and J.R. Sapirstein, Phys. Rev. Lett., 43 (1979) 668.
25. W. Celmaster and R.J. Gonsalves, Phys. Rev. Lett., 44 (1980) 560.
26. C. J. Maxwell and D. G. Tonge, Nucl. Phys., B481 (1996) 681.
27. A. L. Kataev and V. V. Starshenko, Mod. Phys. Lett., A10 (1995) 235.
28. F. LeDiberder, Nucl. Phys. (Proc. Suppl.), B39 (1995) 318.
29. M. Beneke, Nucl. Phys., B405 (1993) 424.
30. P. A. Baikov, K.G. Chetyrkin, and J.H. Kühn, Phys. Rev. Lett., 88 (2002) 012001.
31. B.L. Ioffe and K.N. Zyablyuk, Eur. Phys. J., C27 (2003) 229.
32. S. Bethke, Nucl. Phys. (Proc. Suppl.), 135 (2004) 345.
33. DELPHI Collaboration (J. Abdallah et al.), Eur. Phys. J., C37 (2004) 1.